Supplemental material

Liu et al., https://doi.org/10.1083/jcb.201806205

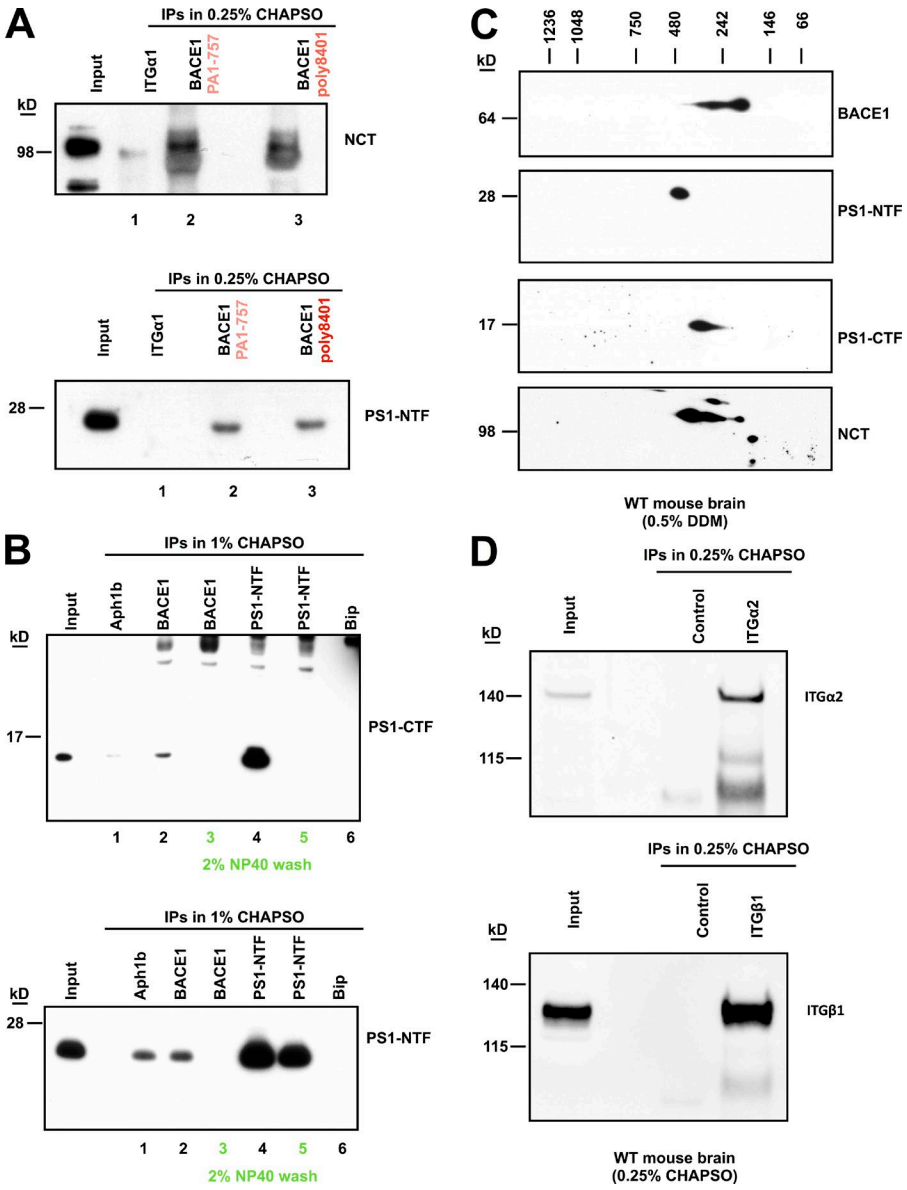

Figure S1. **The β/γ-secretase complex is specific and sensitive to detergent. (A)** 0.25% CHAPSO-solubilized lysates of WT mouse brain microsomes were immunoprecipitated for BACE1 using two different antibodies or ITGα1 as a control. Immunoprecipitates were probed for coIP of the γ components NCT and PS1-NTF. **(B)** 1% CHAPSO-solubilized lysates of WT mouse brain microsomes were immunoprecipitated for BACE1, Aph-1b, PS1-NTF, or Bip as a control. Immunoprecipitates were washed with different detergents: lanes 1, 2, 4, and 6 with 1% CHAPSO, and lanes 3 and 5 with 2% NP-40. **(C)** 0.5% DDM-solubilized lysates of WT mouse brain microsomes were loaded onto BN-PAGE followed by second-dimension SDS-PAGE and immunoblotting for BACE1, PS1-NTF, PS1-CTF, and NCT. **(D)** 0.25% CHAPSO-solubilized lysates of WT mouse brain microsomes were immunoprecipitated for ITGα2 (left panel) or ITGβ1 (right panel), with normal rabbit IgG as a control. Immunoprecipitates were probed for IP of ITGα2 or ITGβ1.

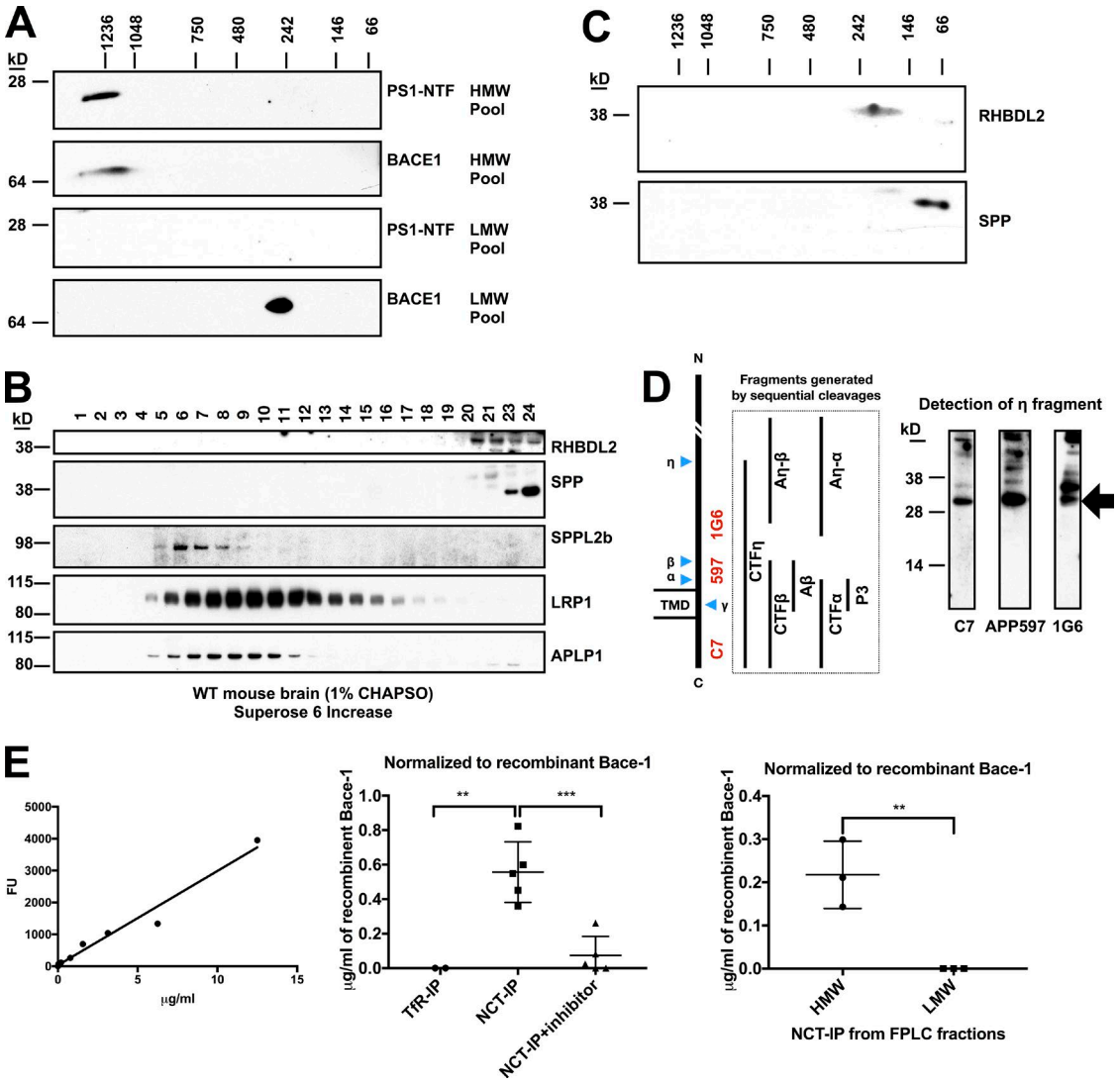

Figure S2. **Distribution of intramembrane proteases in FPLC fractions of mouse brain. (A)** Pooled HMW and LMW FPLC fractions of mouse brain loaded onto BN-PAGE followed by second-dimension SDS-PAGE and blotting for BACE1 and PS1-NTF. **(B)** 1% CHAPSO-solubilized WT mouse brain microsomes were fractionated on a Superose 6 Increase FPLC column and blotted with antibodies to the five indicated proteins. **(C)** 1% CHAPSO-solubilized lysates of WT mouse brain microsomes were loaded onto BN-PAGE followed by second-dimension SDS-PAGE and blotting for RHBDL2 and SPP. **(D)** Schematic of APP fragments generated by certain cleavages. Regional antibodies C7 (to APP676–695), APP597 (to Aβ1–16), and 1G6 (to APP573–576) all recognize an ∼30-kD band (arrow), consistent with it being η-CTF. **(E)** Left: Calibration of a β-secretase activity assay with recombinant human BACE1 as a standard. Middle and right: β-Secretase activity in coimmunoprecipitated complexes from mouse brain lysates (middle) and in pooled FPLC fractions (right graph) were quantified versus standard curve. Data points below the lower end of the standard curve are represented as 0.

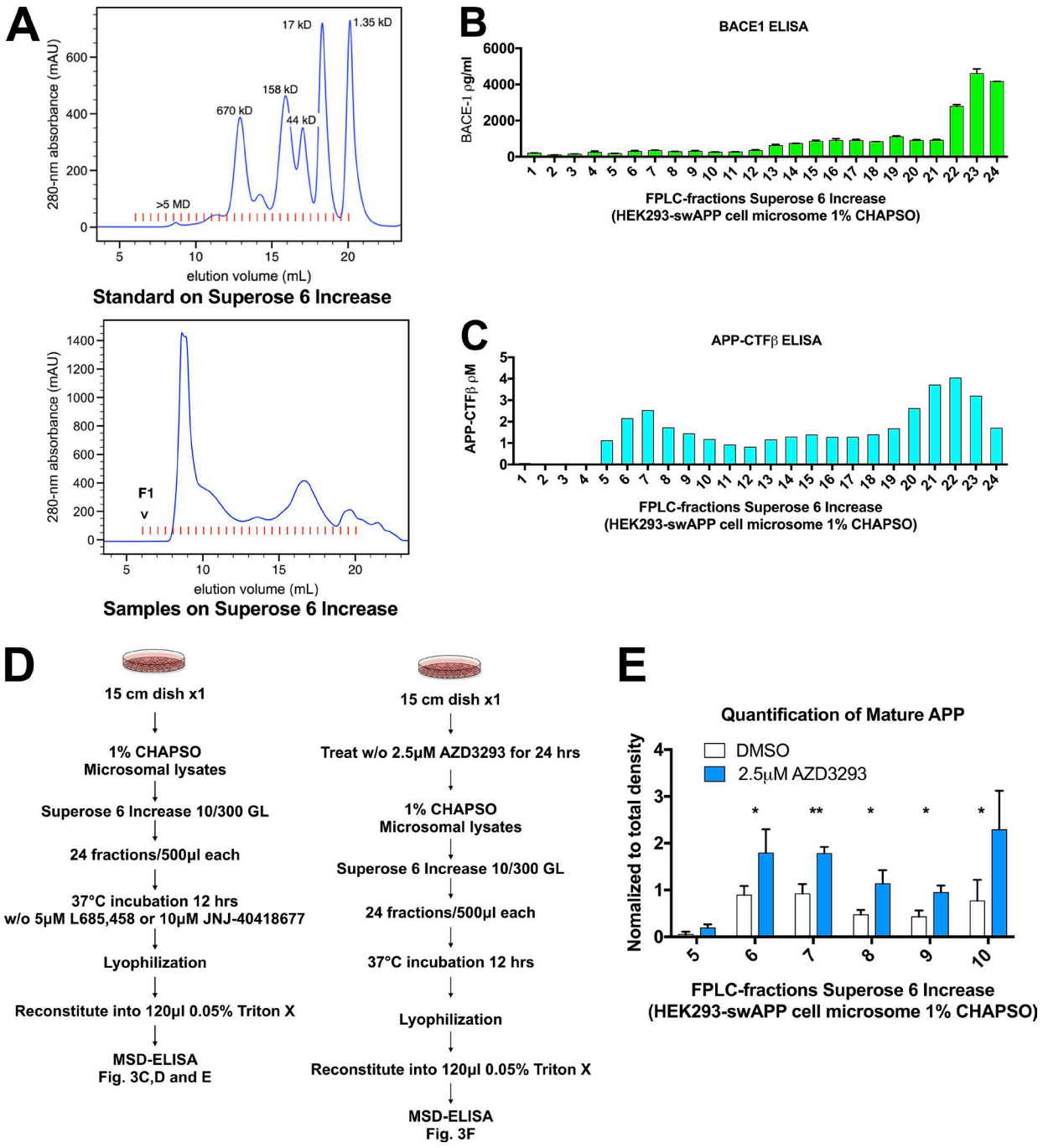

Figure S3. **FPLC fractions from HEK293-swAPP cells: distribution of BACE1, APP-CTFβ, and holo-APP. (A)** Performance of Superose 6 Increase column in separating calibration standards (marked with MWs), and 1% CHAPSO cell microsomes lysate (F1 marks the #1 fraction collected for analysis). **(B)** BACE1 ELISA of FPLC fractions (n = 2; means ± SD). **(C)** APP-CTFβ ELISA of FPLC fractions (n = 1). **(D)** Schematic of the experimental design for de novo Aβ generation using FPLC fractions. Left: Standard protocol. Right: Protocol with pretreatment of cells with the BACE1 inhibitor AZD3293. **(E)** Mature APP levels in FPLC fractions #5–10 of cells treated with AZD3293 versus just DMSO were quantified by densitometry in three independent blots (representative blot is in Fig. 3 G). The density of mature APP signals in each fraction was normalized to the total density of mature APP signals from all fractions on the same blot. n = 3; means ± SD. Unpaired Student's t test: *, P < 0.05; **, P < 0.01.

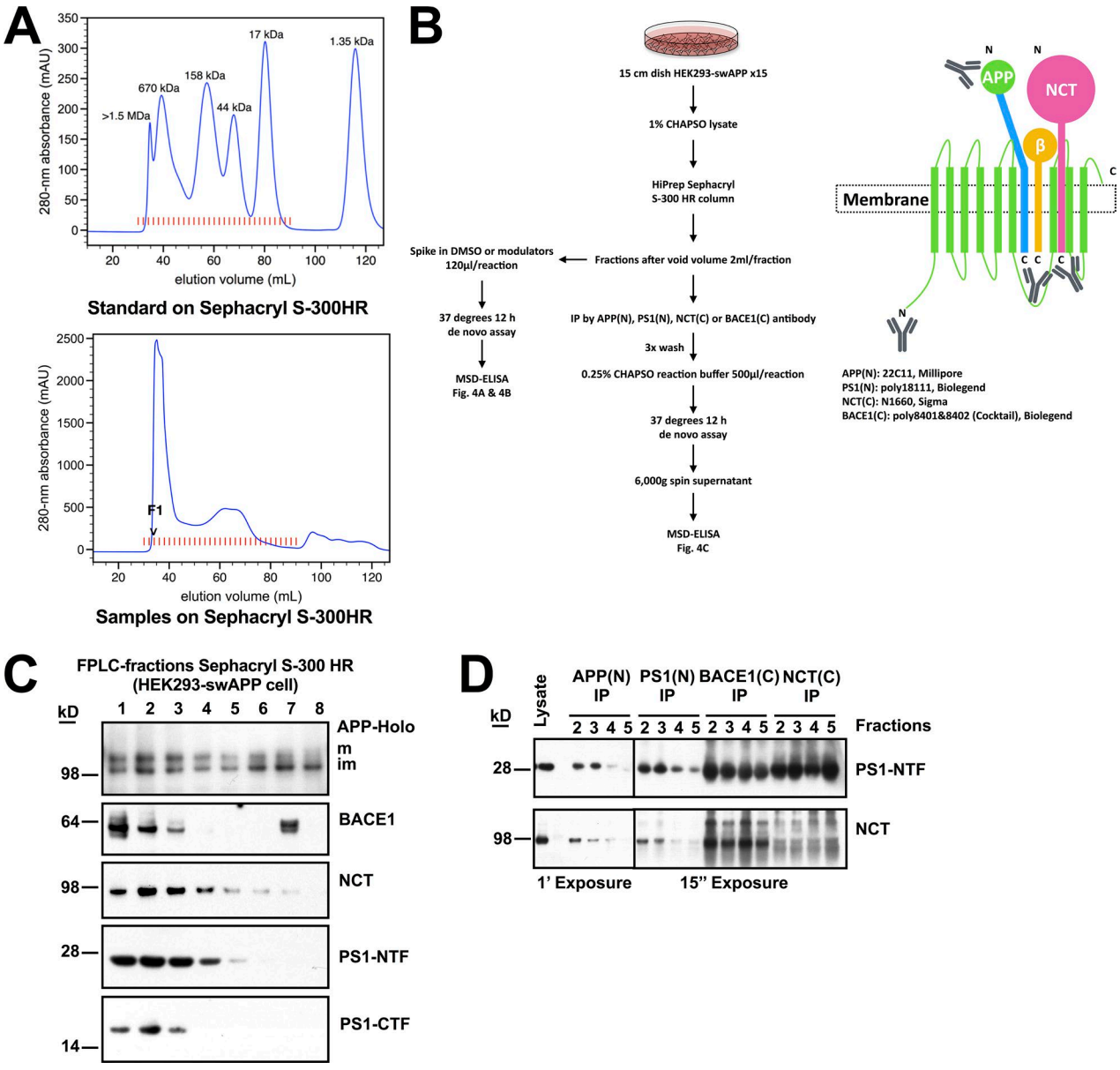

Figure S4. **Catalytically active HMW complexes are isolated by IP. (A)** Performance of Sephacryl S-300 HR columns on separation of calibration standards (marked with MW) and 1% CHAPSO cell microsome lysate (F1 marks the #1 fraction collected for analysis). **(B)** Design of de novo and IP de novo Aβ generation experiments on FPLC fractions. The diagram on the right indicates approximate binding sites of the four antibodies used for IP. **(C)** Immunoblots of APP, BACE1, NCT, PS1-NTF, and PS1-CTF from FPLC fractions #1–8. **(D)** Immunoblots of PS1-NTF and NCT from FPLC fractions #1–8 FPLC immunoprecipitated with APP(N), PS1(N), BACE1(C), and NCT(C) antibodies. Both blots shown are from the same gel; images are from two exposures (1 min and 15 s).

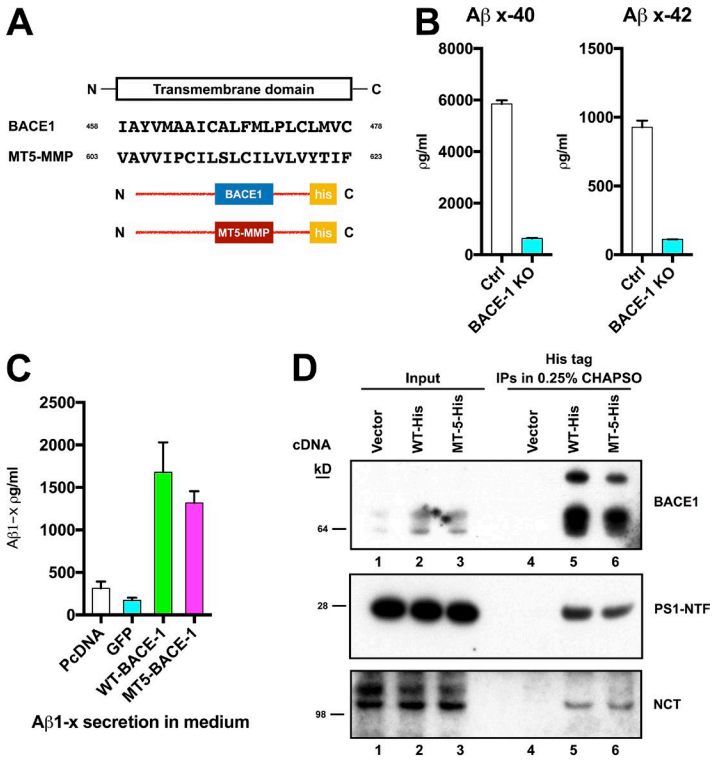

Figure S5. **TMD of BACE1 is not specific for β/γ complex formation. (A)** Comparison of TMD sequences of BACE1 and MT5-MMP and schematic of BACE1 *chimera* with TMD from MT5-MMP. **(B)** Aβx-40 and Aβx-42 were measured in conditioned medium of HEK293-swAPP/BACE1 KO cells versus the parental HEK293-swAPP line as the control (n = 3, means ± SD). **(C)** Aβ1-x was measured in the medium of HEK293/swAPP/BACE1 KO cells transfected with WT-BACE1, MT5-BACE1 with GFP, or empty vector as the control (n = 6, means ± SD). **(D)** IP using anti-His antibody was done in 0.25% CHAPSO-solubilized microsomes from HEK293-swAPP/BACE1 KO cells transfected with WT BACE1 or MT5-BACE1 or with empty vector as the control. Immunoprecipitated samples and input lysates were blotted for BACE1, PS1-NTF, and NCT.